scientific reports

Check for updates

OPEN

Molecular and biological characterization of transforming growth factor-β homolog derived from *Trichinella spiralis*

Salisa Chaimon[1,2,3], Orawan Phuphisut[1], Onrapak Reamtong[4], Sumate Ampawong[5], Kamonpan Fongsodsri[5], Pathanin Chantree[2,3,6], Jeeraphong Thanongsaksrikul[7,8], Preeyarat Malaithong[1], Suthasinee Sreesai[9], Wanchai Maleewong[10,11], Lakkhana Sadaow[10,11], Pongsakorn Martviset[2,3,6]✉ & Poom Adisakwattana[1]✉

The cytokine homologs, particularly transforming growth factor (TGF)-β, is a crucial immunomodulatory molecule and involved in growth and developmental processes in several helminths. In this study, the basic properties and functions of *T. spiralis* TGF-β homolog 2 (TsTGH2) were characterized using bioinformatics and molecular biology approaches. Bioinformatics analyses indicated that TsTGH2 belongs to the TGF-β subfamily. Recombinant TsTGH2 (rTsTGH2) expressed in *Escherichia coli* was used to produce a polyclonal antibody (pAb) in mice. Western blot and immunolocalization using pAb detected native TsTGH2 in crude worm antigens from muscle larvae and adults, showing it was mainly localized in the body wall muscles and the epithelia of the ovary and uterus. To assess the interplay between TsTGH2 and the human TGF-β signaling pathway, rTsTGH2 produced in a HEK293T cell was incubated with the SBE luciferase-HEK293 cell. The result indicated a significant increase in luciferase activity after treatment with rTsTGH2 compared to untreated control ($p < 0.05$). In conclusion, these findings are the first to characterize the basic properties and functions of TGF-β homologs in *T. spiralis*, demonstrating their interaction with the human TGF-β receptor. Further investigation is required to identify and optimize an appropriate expression system or conditions for TsTGH2. Additionally, studies are needed to clarify the specific role of native TsTGH2 in parasite development and host immunomodulation.

Keywords *Trichinella spiralis*, Cytokine homolog, Transforming growth factor-β homolog (TGH), Immunomodulation

Abbreviations

AW	Adult worm
BMP	Bone morphogenetic protein
cDNA	Complementary DNA
CSA	Crude somatic antigen
DCIP	2, 6-dichloroindophenol sodium salt hydrate

[1]Department of Helminthology, Faculty of Tropical Medicine, Mahidol University, Bangkok 10400, Thailand. [2]Department of Preclinical Science, Faculty of Medicine, Thammasat University, Pathumthani 12120, Thailand. [3]Graduate Program in Applied Biosciences, Faculty of Medicine, Thammasat University, Pathumthani 12120, Thailand. [4]Department of Molecular Tropical Medicine and Genetics, Faculty of Tropical Medicine, Mahidol University, Bangkok 10400, Thailand. [5]Department of Tropical Pathology, Faculty of Tropical Medicine, Mahidol University, Bangkok 10400, Thailand. [6]Thammasat University Research Unit in Nutraceuticals and Food Safety, Thammasat University, Pathumthani 12120, Thailand. [7]Graduate Program in Biomedical Sciences, Faculty of Allied Health Sciences, Thammasat University, Pathum Thani 12120, Thailand. [8]Thammasat University Research Unit in Molecular Pathogenesis and Immunology of Infectious Diseases, Thammasat University, Pathum Thani 12120, Thailand. [9]Central Equipment Unit, Faculty of Tropical Medicine, Mahidol University, Bangkok 10400, Thailand. [10]Mekong Health Science Research Institute, Khon Kaen University, Khon Kaen 40002, Thailand. [11]Department of Parasitology, Faculty of Medicine, Khon Kaen University, Khon Kaen 40002, Thailand. ✉email: pong_m@tu.ac.th; poom.adi@mahidol.edu

dpi	Days post-infection
ELISA	Enzyme-linked immunosorbent assay
ES	Excretory-secretory product
HEK293T	Human embryonic kidney 293T cell line
IPTG	Isopropyl β-d-1-thiogalactopyranoside
kDa	Kilodalton
LAP	Latency associated peptide
MIF	Macrophage migration inhibitory factor
ML	Muscle larvae
MW	Molecular weight
NBL	Newborn larvae
pAb	Polyclonal antibody
PBS	Phosphate buffered saline
PC	Proprotein convertase
PEI	Polyethylenimine
pI	Isoelectric point
PSA	Prostate-specific antigen
PVDF	Polyvinyl difluoride membranes
TGF	Transforming growth factor

Background

Trichinella spiralis is a zoonotic nematode that causes trichinellosis in various mammal hosts, including humans. The host becomes infected by ingesting raw or undercooked infected meat. Capsule-forming larvae inside skeleton muscles are released after exposure to gastric juice and migrate to the small intestine, where they mature and reproduce. After copulation, newborn larvae (NBL) are released and migrate through the circulatory system into skeletal muscles for encystation, called nurse cells[1,2]. During *T. spiralis* infection, the parasite and its products interact with the host immune system to escape the immune response[3]. Apart from being beneficial to survival, *T. spiralis* induces some immunoregulatory mechanisms that alleviate the severity of various inflammatory diseases, such as experimental colitis, autoimmune encephalomyelitis, autoimmune type 1 diabetes, and airway allergic inflammation[4–7]. However, some previous clinical trials raised concerns regarding side effects and health risks when using live parasite therapy[8]. Therefore, exploring potential immunomodulatory molecules derived from parasites may be an alternative approach to combat unrelated immune disorders.

Various biomolecules secreted from *T. spiralis*, such as cystatins, serpins, glycans, mucins, lectins, and cytokine homologs, have been identified as potential immunomodulators[9]. The 45 kDa glycoprotein secreted by the first-stage larva *T. spiralis*(gp45) had inhibitory effects on neutrophil function in vitro, suggesting its possible involvement in the decrease of inflammatory cells around the encysted parasite during the acute phase of infection[10]. The recombinant 53 kDa protein of *T. spiralis*(rTsP53) can prevent experimental colitis in immunized mice by stimulating Th2 and suppressing Th1 responses[11]. rTsP53 also protects lipopolysaccharide-induced endotoxemia acute lung injury in a mouse model through the induction of M2 macrophage polarization[12,13]. *T. spiralis* novel cystatin (TsCstN) elicits an anti-inflammatory property by suppressing proinflammatory cytokines and interfering with the antigen-presenting process by depleting major histocompatibility complex class II expression[14]. Moreover, the release of cytokine homologs is an effective mechanism that parasites use to regulate host immunity to facilitate their survival. In *T. spiralis* and *T. pseudospiralis*, a cytokine homolog, namely macrophage migration inhibitory factor, inhibited the migration of mouse and human peripheral blood mononuclear cells[15,16].

The transforming growth factor (TGF)-β superfamily is a large group of proteins that have highly pleiotropic properties in regulating various biological processes, such as growth, development, tissue homeostasis, and immune system regulation, and is found in various animal species, including invertebrates and vertebrates[17]. The members of the TGF-β superfamily can be categorized into two major subfamilies based on sequence homology and specific signaling pathways they activate, including the TGF-β/activin/inhibin subfamily and the bone morphogenetic protein (BMP)/growth differentiation factor/Müllerian inhibiting substance subfamily[18]. In parasitic helminths, TGF-β superfamily members have been identified and characterized in filarial nematodes[19,20], hookworms[21], schistosomes[22,23], and *Fasciola hepatica*[24]. However, the properties and functions of this protein superfamily in *Trichinella* spp., including *T. spiralis*, have not been studied and need to be intensively characterized. A better understanding of the functions of *T. spiralis* TGF-β homolog (TsTGH) will be advantageous for developing novel therapies against inflammatory and immune disorders. Furthermore, TsTGH could serve as a drug and vaccine development target to treat and prevent trichinellosis in humans and animals.

This study aimed to characterize the properties and functions of TGH (TsTGH2) from *T. spiralis* using bioinformatics and molecular biology approaches. The basic functions and properties of TsTGH2 were predicted using several bioinformatics platforms for protein sequence analysis and protein structure simulation. rTsTGH2 was heterologously expressed in the prokaryotic or mammalian system. Native TsTGH2 in the parasite antigen and tissue was determined using immunoblotting and immunohistochemistry, respectively. Furthermore, the interaction between TsTGH2 and TGF-β receptor was analyzed using TGF-β reporter cells.

Methods

Parasites

The mice used in this study were purchased from Nomura Siam International Co., Ltd., Bangkok, Thailand. The maintenance of the *T. spiralis*'s life cycle and all experiments involving the mouse model were conducted at the Laboratory Animal Science Unit of the Faculty of Tropical Medicine (FTM), Mahidol University, Bangkok, Thailand, in accordance with the guidelines of the FTM-Animal Care and Use Committee (ACUC), under approval number FTM-ACUC 018/2021. All animal experiments were conducted in accordance with ARRIVE guidelines. All methods were performed in accordance with relevant guidelines and regulations. Approximately 400 muscle larvae (ML) *T. spiralis* strain ISS62[25] were orally infected into 6- to 8-week-old ICR mice. Adult worms (AWs) were obtained from the intestines of infected mice at 3 and 6 days postinfection (dpi), as described previously[26]. To obtain ML, mice were euthanized at 40 dpi before homogenization in pepsin solution (1% [w/v] pepsin [BDH Ltd., Poole, UK] and 1% [v/v] HCl) and incubated at 37 °C for 1 to 2 h, respectively. After digestion, larvae were separated from host tissue using the Baermann technique[27] and washed thoroughly with 0.85% normal saline solution. Parasites were collected in a microcentrifuge tube and stored at − 80 °C until use.

Preparation of parasite antigens

The crude somatic antigen (CSA) and excretory-secretory (ES) product of *T. spiralis* were prepared, as described previously[14,28]. Briefly, CSA was prepared by homogenizing *T. spiralis* AW (6 dpi) or ML in 1× phosphate-buffered saline (PBS) containing 1% Triton X-100 using a tissue grinder. Subsequently, the homogenate was further homogenized by Sonics Vibra Cell VCX 130 (Sonics & Materials, Inc., Newton, CT, USA) for four cycles, 9 s on/off at 30% amplitude. The supernatant (CSA) was collected after centrifugation at 12,000× *g* for 30 min at 4 °C. To collect the ES product, *T. spiralis* developmental stages (AW and ML) were cultured in RPMI-1640 medium (GE Healthcare Life Sciences, South Logan, UT, USA) in 5% CO_2 at 37 °C for 18 h. Subsequently, the medium containing the ES product was collected, followed by filtering through a 0.2 µm Nalgene syringe filter (Thermo Scientific Nalgene, Rochester, NY, USA) and concentrating using Microsep™ Advance Centrifugal Devices with 3 K Omega (Pall Life Sciences, Port Washington, NY, USA). Protein concentration was measured by Pierce™ BCA Protein Assay Kit (Thermo Fisher Scientific, Inc., Bannockburn, IL, USA) according to the manufacturer's instructions.

Bioinformatics analysis

The full-length nucleotide and deduced amino acid sequences of TsTGH2 were obtained from the National Center for Biotechnology Information (GenBank nos. FJ513372.1 and ACT10102.1, respectively). The deduced amino acid sequence was used to predict protein properties, including molecular weight (MW) and isoelectric point (pI) using EMBOSS Pepstats[29], signal peptide using SignalP 5.0 Server[30], transmembrane regions using TMHMM Server version 2.0[31], N- and O-glycosylation sites using NetNGlyc 1.0 and NetOGlyc 4.0 Server[32,33], and furin cleavage site using ProP 1.0 Server[34]. Additionally, percentage identity and similarity between TsTGH2 and other homologs belonging to the TGF-β superfamily were determined using the BLASTP and Ident and Sim programs[35].

The conserved protein motifs and consensus residues of mature-TsTGH2 (mTsTGH2) were compared to homologs belonging to the TGF-β superfamily using MUSCLE[36]. Phylogenetic analysis was conducted using a maximum likelihood method with 1,000 bootstrap replications in MEGA 11[37]. The accession numbers of all sequences used in this study are shown in Supplementary Information File 1: Table S1.

The two-dimensional (2D) structure of TsTGH2 was predicted using the PDBsum server[38]. The three-dimensional (3D) structure of TsTGH2 was simulated by the I-TASSER server[39] using the highest homology crystal structure of *Sus scrofa* TGF- β1 as a template (PDB ID: 3rjrA). Subsequently, the predicted 3D model was refined protein structure to improve the structure quality using the GalaxyRefine server[40]. To validate the refined 3D structure of TsTGH2, a Ramachandran plot was generated using the MolProbity server[41]. Moreover, the overall model quality of TsTGH2 was further validated using the PROSA server. If an overall quality score (Z-score) is outside the range characteristic for native proteins, it indicates an erroneous structure[42].

Production of rTsTGH2 protein in the prokaryotic expression system

Total RNA was isolated from *T. spiralis* ML using Trizol reagent (Invitrogen, Carlsbad, CA, USA) according to the manufacturer's instructions. The first-strand cDNA was constructed from total RNA using the RevertAid First Strand cDNA Synthesis Kit (Thermo Fisher Scientific) and used as the template DNA to amplify pro-TsTGH2 (pTsTGH2) and mTsTGH2. The specific primers of pTsTGH2 and mTsTGH2 were designed and incorporated with *Hin*dIII and *Xho*I for cloning into the pET20b$^+$ bacterial expression vector (Supplementary Information File 1: Table S2). The polymerase chain reaction (PCR) product was amplified using Taq polymerase (Thermo Fisher Scientific) under the following conditions: at 94 °C for 5 min; followed by 35 cycles of 94 °C for 30 s, 50 °C for 30 s, and 72 °C for 1 min; and a final step of 72 °C for 5 min. The PCR product was cloned into pET20b$^+$ and used in protein expression experiments.

The recombinant plasmid pET20b$^+$ containing pTsTGH2 or mTsTGH2 was transformed into *Escherichia coli* BL21 (DE3) pLysS using the heat-shock transformation method[28]. Recombinant pTsTGH2 (rpTsTGH2) and mTsTGH2 (rmTsTGH2) expression was induced by 0.5 mM isopropyl β-D-1-thiogalactopyranoside (IPTG) for 3 h at 37 °C. Bacterial cells were harvested and resuspended in lysis buffer (6 M guanidine), followed by purification of the recombinant proteins using a Talon Metal Affinity Resin column (Clontech Laboratories, Inc., Mountain View, CA, USA) under denaturing conditions, as described previously[28,43]. All eluted fractions were examined using 12% sodium dodecyl sulfate-polyacrylamide gel electrophoresis (SDS-PAGE) and stained with Coomassie brilliant blue G-250. The purified rTsTGH2 was pooled and dialyzed against 1× PBS before immunization for mice (purchased from Nomura Siam International Co.,Ltd., Bangkok, Thailand) to produce

polyclonal antibody (pAb), as described previously, with some modifications[28]. Briefly, 20 µg purified rmTsTGH2 containing an equal volume of Imject Alum (Thermo Fisher Scientific) was intraperitoneally injected into three mice as the primary injection, followed by three boosts of 20 µg in Imject Alum on days 14, 28, and 32. Blood was collected 1 week after the third booster, and serum was obtained and stored at − 20 °C until use. According to a previous publication, the antibody titer and specificity of mouse anti-rmTsTGH2 pAb were determined using indirect enzyme-linked immunosorbent assay (ELISA) and immunoblotting[44,45].

Detection of TsTGH2 in parasite antigens and tissues

CSA, ES product, rpTsTGH2, and rmTsTGH2 were size separated by 12% SDS-PAGE and electrically transferred onto polyvinylidene difluoride membranes (Pall Corp., Port Washington, NY, USA). The membranes were blocked with 5% skimmed milk in 1× PBS containing 0.05% Tween 20 (PBST) at room temperature (RT) for 1 h. To detect native TsTGH2, the membrane was washed thrice with PBST and incubated with a 1:100 dilution of preimmunization sera or mouse anti-rmTsTGH2 pAb at 4 °C overnight. After washing thrice with PBST, the membrane was incubated with 1:2000 horseradish peroxidase (HRP)-conjugated goat anti-mouse IgG (Southern Biotech, Birmingham, AL, USA) at RT for 1 h. The bands were visualized by adding 2,6-dichloroindophenol sodium salt hydrate substrate (Sigma-Aldrich Co., St. Louis, MO, USA).

Immunolocalization was performed according to a previous publication with some modifications[28]. In summary, 5 µm paraffin-embedded sections of the developmental stages of *T. spiralis*(AW-3dpi, AW-6dpi, and ML) were deparaffinized and rehydrated, antigenic epitopes were retrieved, and endogenous peroxidase was inactivated before blocking with blocking solution (10% fetal bovine serum [FBS] in 1× PBS, pH 7.4). The sections were subsequently incubated with mouse anti-rmTsTGH2 (1:100) or preimmune sera (1:100) at 4 °C overnight in a humidified chamber and conjugated with HRP-conjugated goat anti-mouse IgG (1:1,000; Southern Biotech). The colorimetric signal was developed using the AEC staining kit (Sigma-Aldrich) according to the manufacturer's instructions, followed by counterstaining with hematoxylin solution modified according to Gill III (Sigma-Aldrich) and 0.1% sodium bicarbonate. The sections were mounted and visualized using a Nikon Eclipse Ci series microscope (Nikon Co., Tokyo, Japan).

Production of rTsTGH2 protein in the mammalian expression system

The protein sequences encoding pTsTGH2 and mTsTGH2 were employed for codon optimization to enhance gene expression in the human embryonic kidney 293T (HEK293T) cell line using the GenSmart Optimization tool[46]. The optimized DNA sequences of pTsTGH2 and mTsTGH2 were synthesized using a gene synthesis service (U2Bio [Thailand] Co., Ltd, Bangkok, Thailand) and cloned into the pUC57 vector. After synthesis, the DNA fragments were subcloned into pSecTag2A (Thermo Fisher Scientific) at the *Hin*dIII and *Xho*I restriction sites. The pSecTag2/human prostate-specific antigen (hPSA) vector (Invitrogen) is a positive control for assessing expression and secretion in the HEK293T cell line.

For recombinant protein expression, HEK293T cells (Lenti-X HEK293T) were cultured in Dulbecco's modified Eagle's medium (DMEM; Cytiva HyClone Laboratories, Logan, UT, USA) containing 100 U m/mL penicillin, 100 mg/mL streptomycin, and 5% FBS at 37 °C with 5% CO_2 until reaching 80% confluence before plating into six-well culture plates at a density of 5×10^5 cells per well. The following day, each recombinant plasmid (pSecTag2/pTsTGH2, pSecTag2/mTsTGH2 or pSecTag2/hPSA) was mixed with polyethyleneimine (PEI; Sigma-Aldrich), followed by adding the PEI::DNA complexes into cells and incubating at 37 °C with 5% CO_2 for 24 h. The medium was changed, replaced with CDM4HEK293 medium (Cytiva HyClone Laboratories) containing 100 U/mL penicillin, 100 mg/mL streptomycin, and 2× GlutaMAX™ (Thermo Fisher Scientific), and incubated at 37 °C with 5% CO_2 for up to 4 days. Cells were harvested and mixed with lysis buffer (50 mM NaH_2PO_4, 300 mM NaCl, 10 mM imidazole, 0.05% Tween 20 [pH 8.0]) before breaking using an ultrasonic processor (Vibra cell, Sonics, Newtown, CT, USA) at 30% amplitude with 15 s on/off pulse for 5 min. The cell lysate was centrifuged at 14,000× *g*, 30 min at 4 °C, and purified using a Talon Metal Affinity Resin column (Clontech Laboratories) under native conditions. Purified rpTsTGH2, rmTsTGH2 and rhPSA were dialyzed against 1× PBS, concentrated using Microsep™ Advance Centrifugal Devices with 3 K Omega, and used for the luciferase reporter assay.

Determination of the luciferase reporter assay for TGF-β activity

The SBE luciferase reporter stable HEK293 cell line (ATCC, CRL-1573) (SBE Reporter-HEK293) was developed using a protocol modified from the Data Sheet SBE Luciferase Reporter Lentivirus (TGFβ/SMAD Pathway; BPS Bioscience, San Diego, CA, USA) and Addgene: Virus Protocol-Generating Stable Cell Lines with Lentivirus[47]. In detail, the SBE Luciferase Reporter Lentivirus (BPS Bioscience) was combined with DMEM containing 10% FBS and 10 µg/mL polybrene (EMD Millipore Corp., Darmstadt, Germany) to create a series of virus dilutions (1:20, 1:100, and 1:200) in a final volume of 500 µL, followed by adding each dilution into each well of a six-well culture plate. Reverse transduction was performed by seeding 1 mL HEK293 into each well containing different virus dilutions to a final density of 5×10^4 cells/mL. After 48 h virus incubation on cells, the medium was removed. Cells were given fresh DMEM containing 10% FBS and 2 µg/mL puromycin and incubated for 7 days. Cells that survived after selection with puromycin were used to determine TsTGH2 activating human TGF-β signaling pathway.

One hundred microliters of SBE Reporter-HEK293 cells/well (3.5×10^4 cells) were seeded into white opaque 96-well microplates and incubated at 37 °C with 5% CO_2 overnight. The following day, the medium was removed and changed to an assay medium (DMEM, 0.5% FBS, and 1× GlutaMAX™). Different rpTsTGH2 concentrations (1 and 10 µg/mL), rhPSA (10 µg/mL; irrelevant control) or hTGF-β (2 ng/mL) were added to cells and incubated at 37 °C for 18 h. After incubation, a luciferase assay was performed using the ONE-Step™ Luciferase assay kit

according to the manufacturer's instructions (BPS Bioscience). Luminescence was measured using an Infinite M Plex multimode plate reader (Tecan Group Ltd., Männedorf, Switzerland).

Results were statistically analyzed using GraphPad Prism 6 (GraphPad Software, Inc., La Jolla, CA) and the unpaired t-test to determine the significant differences between each test group and the negative control. Individual data and the mean ± standard deviation of each group are presented. $p < 0.05$ was considered statistically significant. The experiments were performed in triplicate and repeated three times.

Results

Bioinformatics analysis predicted the properties and functions of TsTGH2

Sequence analysis of the full-length TsTGH2 cDNA demonstrated that it consists of 1,269 nucleotides encoding a protein of 423 amino acid residues (aa), with MW of ~47.8 kDa and pI of 8.0. The prediction of potential secretion of TsTGH2 revealed that it contained an N-terminal signal peptide located at amino acid residues 1 to 23 (aa_{1-23}; Sec score = 0.8268), which showed the cleavage site between positions A_{23} and I_{24} (IDA-IG). The domain after cleavage of the signal peptide is called latency-associated peptide (LAP) or pTsTGH2 (aa_{24-432}) and has a predicted molecular mass and pI of ~45 kDa and 7.9, respectively. No transmembrane helix was predicted in this protein. Five potential *N*-glycosylation sites were predicted in TsTGH2 at residues N_{32}, N_{76}, N_{149}, N_{189}, and N_{208}, whereas 11 potential *O*-glycosylation sites were predicted at residues S_{79}, T_{83}, S_{84}, S_{188}, S_{266}, S_{267}, S_{272}, T_{285}, S_{305}, T_{306}, and S_{307} (Supplementary Information File 2: Fig. S1). The proprotein convertase (PC) cleavage motif (RPKR; score = 0.933; cutoff score = 0.5) was found in TsTGH2, which generated mTsTGH2 ($aa_{272-423}$) at MW of 17.2 and pI of 7.4 (Fig. 1A; Supplementary Information file 2: Fig. S1). A search of the full-length amino acid sequence homology of TsTGH2 with homologs revealed that TsTGH2 is most similar (98.58%) and most identical (98.11%) to the *Trichinella* T9 inhibin B chain (T9INHB-B). Inhibin members of other *Trichinella* species are next (72–96% identity and 77–98% similarity), whereas there is less homology to other organisms, including humans (< 14% identity and 29% similarity; Supplementary Information File 1: Table S3).

Multiple sequence alignment was analyzed to identify conserved motifs and consensus residues of mTsTGH2 compared to representative members of the TGF-β superfamily, including BmTsTGH2, CeDAF7, HpTGH2,

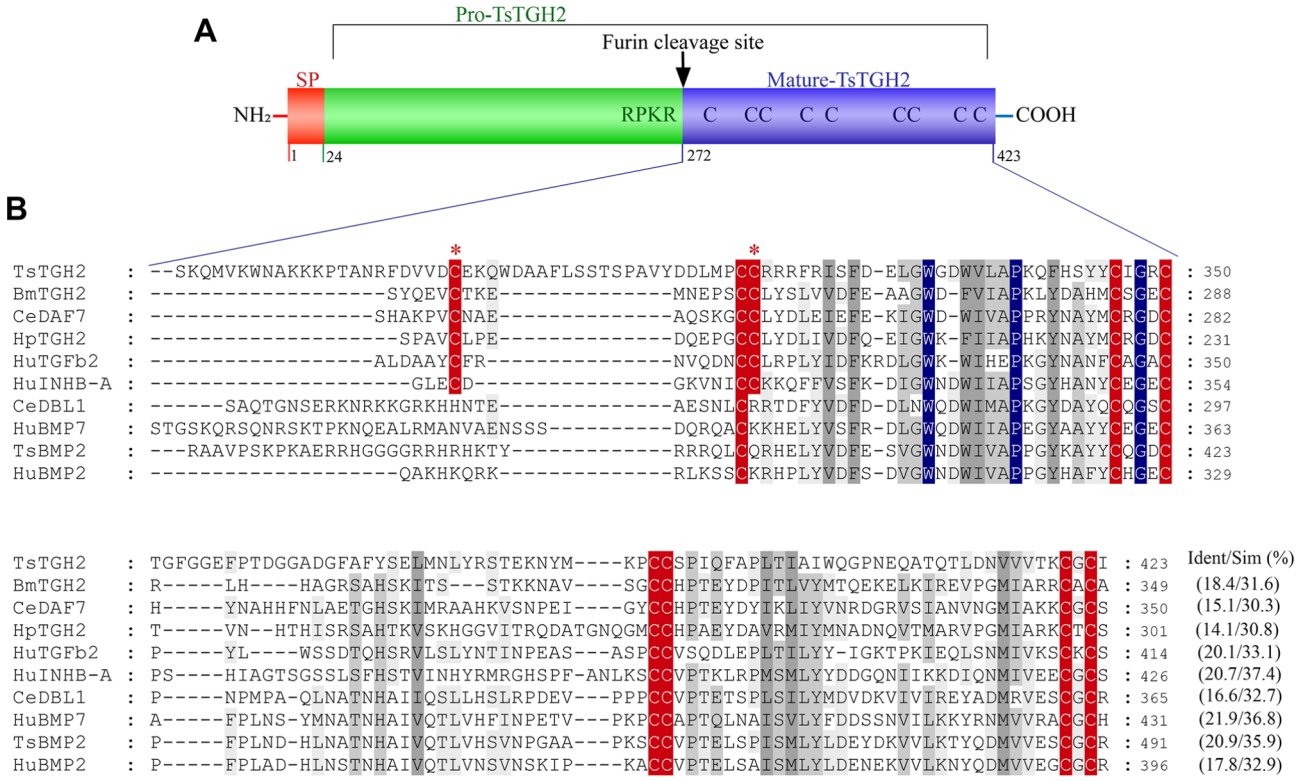

Fig. 1. Schematic of TsTGH2 protein and multiple sequence alignment of TsTGH2 with homologs. (**A**) Domain structure of TsTGH2 consists of signal peptide (amino acid residues (aa) $_{1-23}$), pro-TsTGH2 (pTsTGH2) (aa_{24-423}) containing proteolytic cleavage site motif, RPKR, and mature-TsTGH2 (mTsTGH2) ($aa_{272-423}$) with nine cysteines (C) inside domain. The arrow indicates the furin cleavage site. (**B**) The deduced amino acid sequence of mTsTGH2 was aligned with TGF-β superfamily members from other representatives using MUSCLE. The conserved cysteine residues among TGF-β superfamily are shaded in red and additional conserved residues (tryptophan [W], proline [P], and glycine [G]) are shaded in blue. The stars indicate two of conserved cysteines found only in TGF-β/activin/inactivin subfamily. Gaps are represented with a dash (-). Ident/Sim (%) represents percent identity and similarity between TsTGH2 and each representative sequence. The GenBank accession numbers of the sequence are provided in Supplementary Information File 1: Table S1.

HuTGFb2, HuINHB-A, CeDBL1, HuBMP7, TsBMP2, and HuBMP2 (Fig. 1B). These findings demonstrated that mTsTGH2 is less homologous with these homologs, having low identity and similarity of amino acid sequences at 14–21% and 30–37%, respectively (Fig. 1B). However, mTsTGH2 contained seven conserved cysteine (C) residues, which are major characteristics and necessary for the tertiary structure and dimerization of TGF-β superfamily. TsTGH2 also contained two additional conserved cysteines (C), found only in members of TGF-β, DAF7, activin, and inhibin subfamily but not in the BMP subfamily. Additional conserved residues of tryptophan (W), proline (P), and glycine (G) were also found among TsTGH2 and selected TGF-β superfamily members (Fig. 1B).

A phylogenetic tree was constructed from multiple sequence alignments of full-length TsTGH2 and TGF-β superfamily homologs. The tree revealed that TsTGH2 was clustered in TGF-β/activin/inhibin subfamily clade and most closely related to *Echinococcus multicularis* activin (EmAct), *Schistosoma mansoni* inhibin/activin (SmInAct), and *F. hepatica* inhibin (FhINHB-B; Fig. 2). Moreover, TsTGH2 was also clustered in the same clade with inhibin-β and TGF-β from humans but separated in a different branch.

Structure modeling of TsTGH2

The 2D structure modeling of TsTGH2 by the PDBsum server showed that this protein contained 4 β-sheets (12 strands), 3 β-hairpins, 10 helices, 5 helix-helix interactions, 67 β-turns, 19 γ-turns, and 3 disulfide bonds (Supplementary Information File 2: Fig. S1). The 3D structure of TsTGH2 was modeled by the I-TASSER server. The model was predicted using the crystal structure of *S. scrofa* TGF-β1 (PDB ID: 3rjrA) as the best template. The 3D structure consisted of three domains: signal peptide domain, pTsTGH2, and mTsTGH2 (Fig. 3A). The mTsTGH2 domain contains nine cysteine residues. Six cysteine residues formed three intrachain disulfide bridges with the connectivity of C_{317}–C_{388}, C_{346}–C_{420}, and C_{350}–C_{422}, forming a "cysteine knot" structural motif (Fig. 3B). Moreover, this covalent knot holds a polypeptide fold in which two pairs of antiparallel β-strand (fingers) project away from a short α-helix. This structure can be described as a four-digit hand, with each β-strand as a finger. At the N-terminus, fingers 1 and 2 are antiparallel, with finger 2 leading to the helix (wrist region), followed by antiparallel fingers 3 and 4 at the C-terminus. The cysteine knot region was likened to the palm of the hand (Fig. 3B).

The confidence of the 3D structure predicted by the I-TASSER server was quantitatively measured by C-score. It is calculated based on the significance of threading template alignments and the convergence parameters of the structure assembly simulations. The C-score of the TsTGH2 3D model was −1.64 (typical range: −5 to 2), indicating that the model has good quality and high confidence. The predicted 3D model was refined and validated by GalaxyRefine and MolProbity server. Results revealed that 86.7% of all residues were in favored regions, 11.64% in allowed regions, and 1.66% in disallowed regions, indicating a high quality of the predicted structure (Supplementary Information File 2: Fig. S2A). Moreover, the overall model quality was analyzed by ProSA. Results showed a Z-score of −5.7, within the scores typically found for native proteins (Supplementary Information File 2: Fig. S2B).

Production of rTsTGH2 protein in the bacterial expression system

Recombinant proteins of pTsTGH2 and mTsTGH2 were successfully expressed in the bacterial expression system. However, both forms were expressed as insoluble proteins at MWs of ~45 kDa (Fig. 4A) and 17 kDa (Fig. 4B), respectively. Western blotting analysis of rpTsTGH2 and rmTsTGH2 with mouse anti-His tag antibodies confirmed that both were detected only in the IPTG-induced bacterial lysate, not in the non-induction control (data not shown). rpTsTGH2 and rmTsTGH2 were purified under denaturing conditions, followed by the analysis of the purification results using SDS-PAGE and Western blotting with anti-His tag antibodies. Results showed that purified rpTsTGH2 and rmTsTGH2 were present at MWs of 45 and 17 kDa, respectively, in SDS-PAGE and detected with anti-His tag antibodies at the expected size in Western blotting (Fig. 4A and B). Purified rpTsTGH2 and rmTsTGH2 were stepwise dialyzed to remove urea, and rmTsTGH2 was used for immunizing mice to produce mouse anti-rmTsTGH2 pAb.

The antibody titer and specificity of mouse anti-rmTsTGH2 pAb were determined using ELISA and Western blotting, respectively. ELISA indicated that rmTsTGH2 stimulated antibody response with a high titer (25,600–51,200) in all mice (data not shown). For specificity, mouse anti-rmTsTGH2 pAb specifically reacted to rpTsTGH2 and rmTsTGH2 but showed no reaction with the bacterial cell lysate carrying pET20b$^+$ before or after IPTG induction in Western blotting (Supplementary Information File 2: Fig. S3).

Detection of native TsTGH2 in parasite antigens and tissues

The mouse anti-rmTsTGH2 pAb mentioned above was used to detect native TsTGH2 in parasite antigens, including CSA and ES products of AW-3dpi, AW-6dpi, and ML, using immunoblot analysis. Results revealed that TsTGH2 was mainly detected in the CSA of adult and ML parasites at MWs of ~45 kDa (Fig. 5). Additionally, TsTGH2 was also detected in the ES product of AW-6dpi, but not ML and AW-3dpi, and the band was similar to the MWs of CSA and rpTsTGH2 (45 kDa; Fig. 5). Preimmunized sera did not react with either the CSA or ES product of the parasite (data not shown).

To determine the locations of native TsTGH2 expression in the parasite tissue, immunohistochemistry was performed on the tissue sections of AW-3dpi, AW-6dpi, and ML. After reacting with mouse anti-rmTsTGH2 pAb, TsTGH2 was localized in the body wall muscle (mu) of ML, but not stichosome (st) and genital primordium (gp) (Fig. 6). In AWs, TsTGH2 was detected in the body wall muscle (mu), nucleus (nu) of a body wall muscle (mu), intestine (in), epithelia of the ovary (ov), uterus (ut), hemolymph (hm) and newborn larva (NBL) but not in embryo (em) (Fig. 7). Immunolocalization with preimmune sera (negative control) was negative (Figs. 6 and 7).

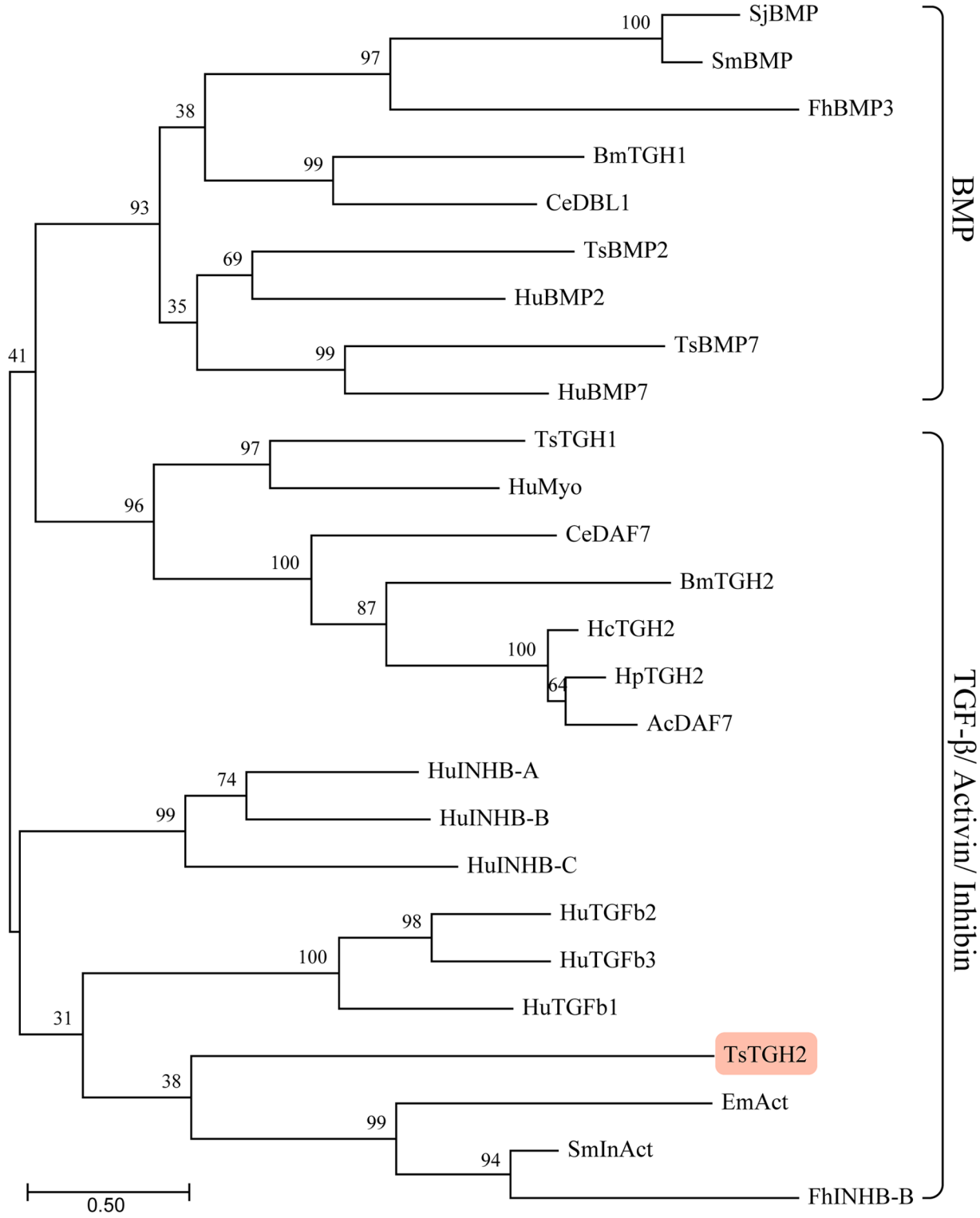

Fig. 2. Phylogenetic relationships between full-length of TsTGH2 and other TGF-β superfamily homologs. The tree was constructed with maximum likelihood method using MEGA11 program, 1,000 bootstrap replicates. TsTGH2 was clustered in TGF-β/activin/inactivin subfamily but not in BMP subfamily. Numbers at the nodes represent the bootstrap values. The abbreviations used and GenBank accession numbers are provided in Supplementary Information File 1: Table S1.

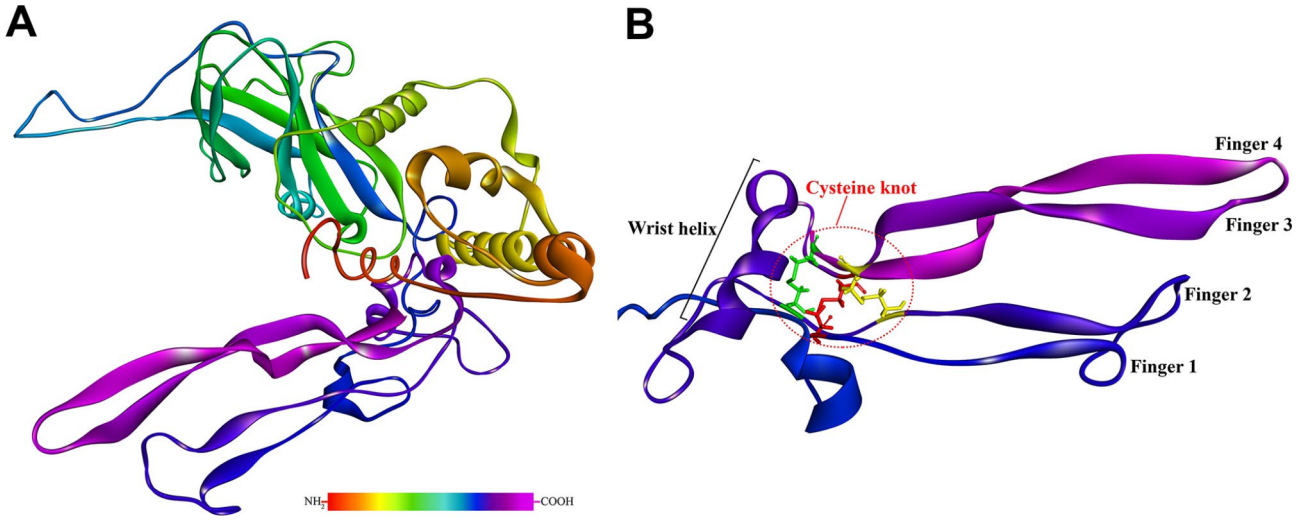

Fig. 3. The predicted 3D structure of TsTGH2. (**A**) The 3D structure of full-length TsTGH2 was modelled and refined by I-TASSER and GalaxyRefine server using the crystal structure of *Sus scrofa* TGF- β1 (PDB ID: 3rjrA) as the template. (**B**) The 3D structure of mature-TsTGH2, consisting cysteine knot (indicated by a red circle) with two pairs of antiparallel β-strands (fingers) extending from wrist helix. Three intrachain disulfide bridges between cysteines are shown in stick format: C_{317}–C_{388} (red stick), C_{346}–C_{420} (yellow stick), and C_{350}–C_{422} (green stick).

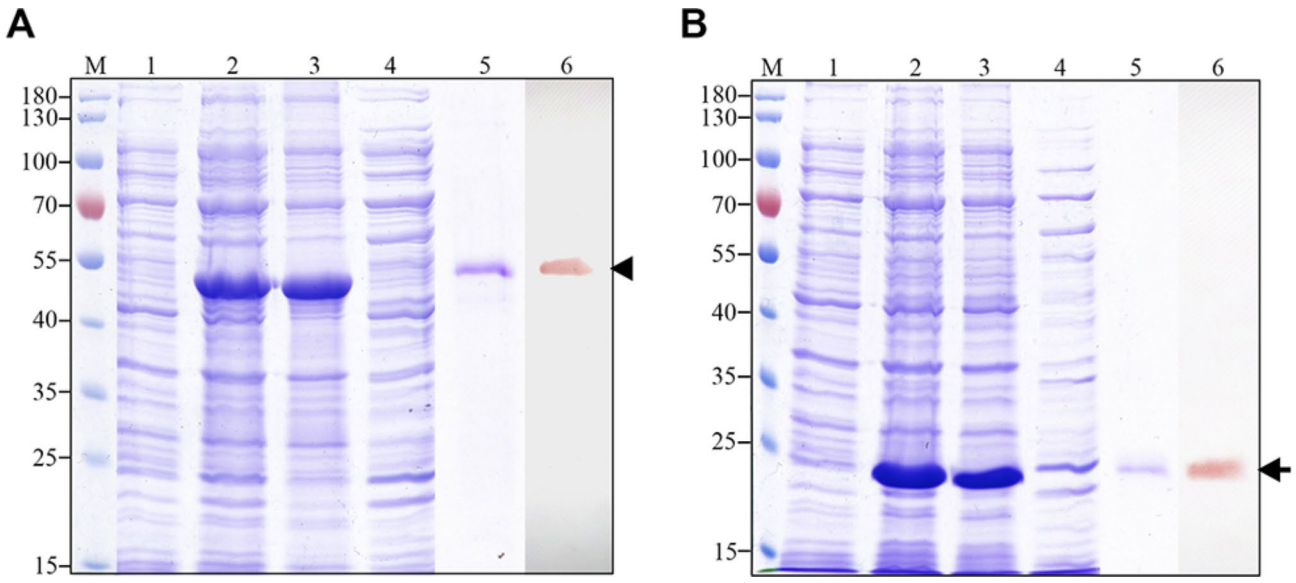

Fig. 4. Expression of rTsTGH2s in prokaryotic expression system. **(A)** recombinant pro-TsTGH2 (rpTsTGH2) and **(B)** recombinant mature-TsTGH2 (rmTsTGH2) were successfully expressed in *E. coli*. Lane M: PageRuler Prestained Protein Ladder (Thermo Fisher Scientific Inc.); Lane 1: non-induction; Lane 2: IPTG induction; Lane 3: insoluble fraction; Lane 4: soluble fraction; Lane 5: purified rTsTGH2; Lane 6: western blot analysis of rTsTGH2 probe with mouse anti-His tag antibody. Arrowhead and arrow indicate rpTsTGH2 and rmTsTGH2, respectively.

Production of rTsTGH2 protein in the mammalian expression system

To facilitate the transfer of recombinant protein production to a culture medium in a mammalian expression system, rpTsTGH2 and rmTsTGH2 cDNAs were cloned after the secretory signal sequence (Igκ leader) of the pSecTag2A vector. Nonetheless, results demonstrated that HEK293T intracellularly expressed rpTsTGH2 and rmTsTGH2 at MWs of ~70 and 20 kDa, respectively, but were not secreted into the culture medium (Fig. 8A and B). HEK293T cells carrying pSecTag2/PSA, serving as a positive control, exhibited rhPSA expression with an MW of ~36 kDa. This expression was detected using mouse anti-His tag antibodies intracellularly and in the culture medium (Fig. 8A and B). rpTsTGH2 and rmTsTGH2 proteins were purified from the HEK293T

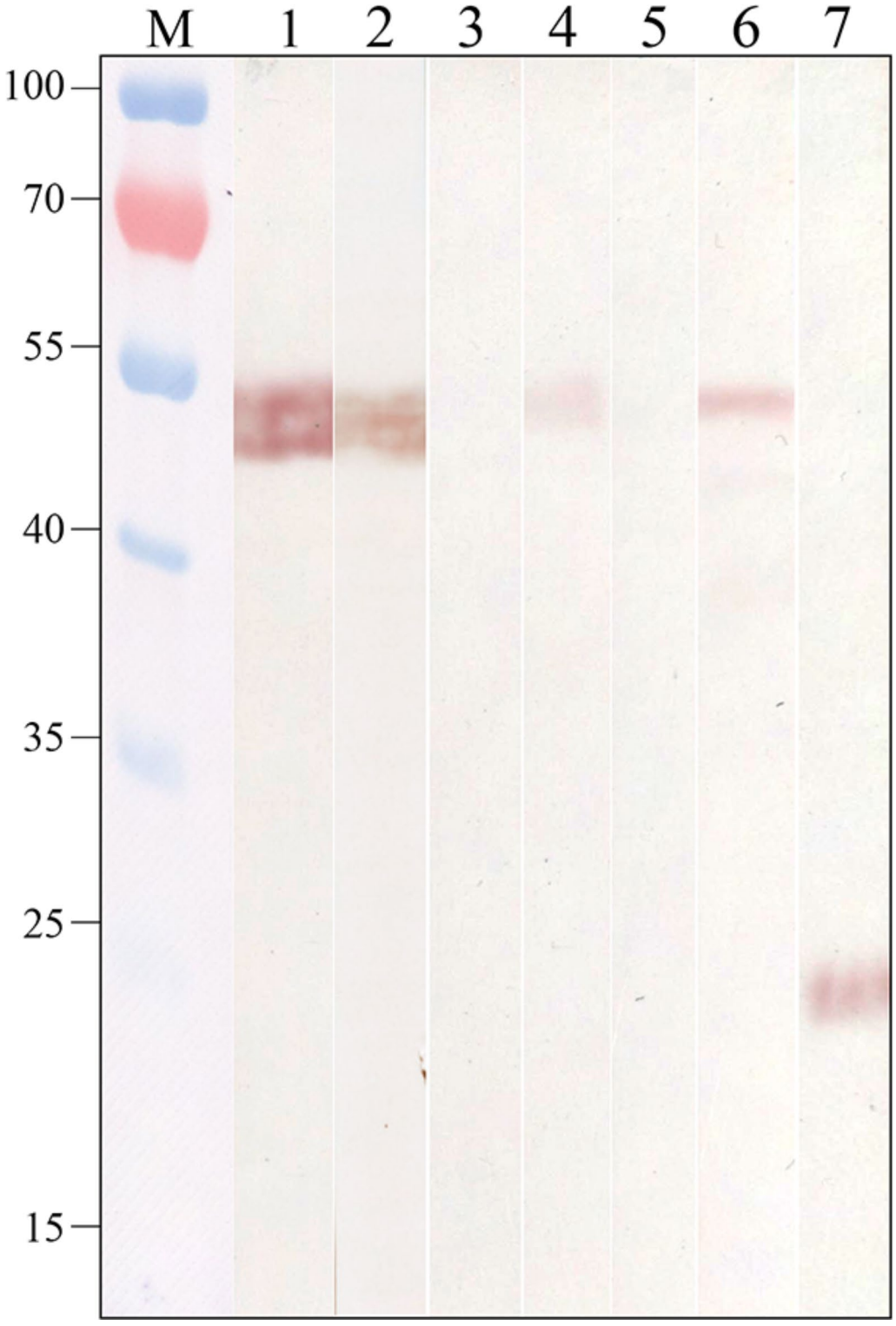

Fig. 5. Detection of native TsTGH2 in parasite antigens. Mouse anti-recombinant mature-TsTGH2 (rmTsTGH2) pAb detected native TsTGH2 in CSA of adult and ML and ES of adult after 3- and 6-day post-infection (dpi). M: PageRuler Prestained Protein Ladder (Thermo Fisher Scientific Inc.); Lane 1 and 2: CSA of adult and ML, respectively; Lane 3 and 4: ES product of adult after 3-dpi and 6-dpi, respectively; Lane 5: ES product of ML; Lane 6: rpTsTGH2; and Lane 7: rmTsTGH2.

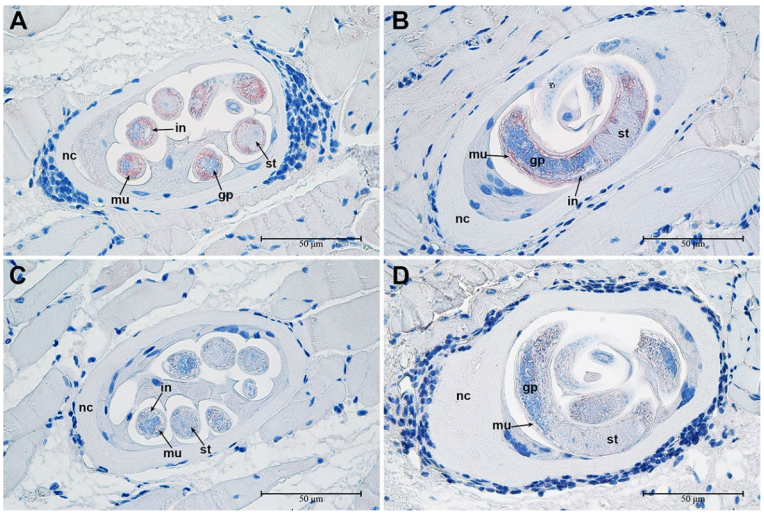

Fig. 6. Immunohistochemical analysis of native TsTGH2 in *T. spiralis* muscle larvae. The red color indicates the tissue localization of native TsTGH2 with mouse anti-rmTsTGH2 pAb (**A** and **B**). Control tissues of *T. spiralis* muscle larvae was reacted with mouse preimmune sera (**C** and **D**). Abbreviations: nc: nurse cell; mu: muscle; in: intestine; gp: genital primordium; st: stichocyte.

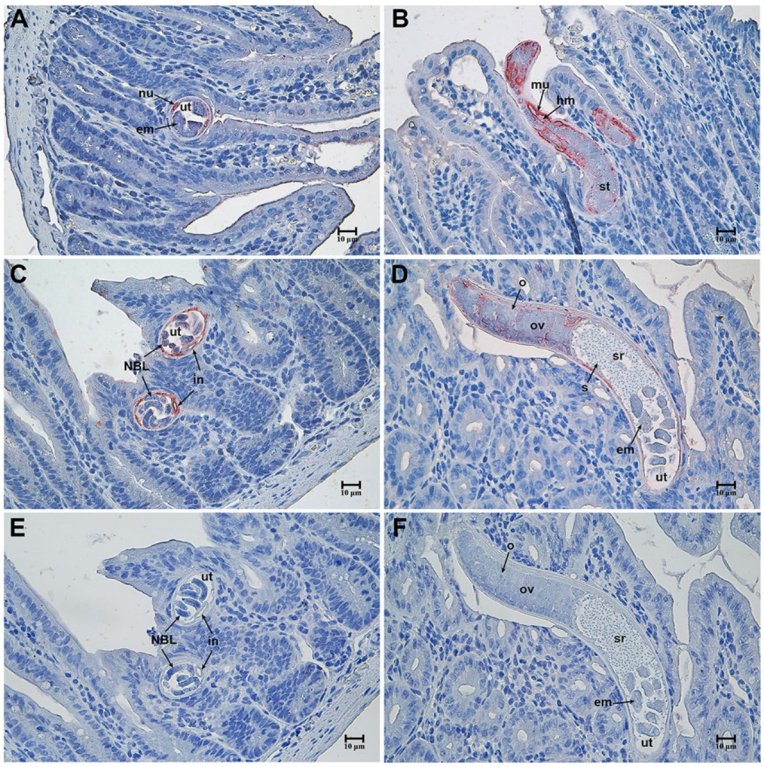

Fig. 7. Immunohistochemical analysis of native TsTGH2 in *T. spiralis* adult stage after 3dpi (**A** and **B**) and 6dpi (**C**–**F**). The red color indicates the tissue localization of native TsTGH2 with mouse anti-rmTsTGH2 pAb (**A**–**D**). Control tissue of *T. spiralis* adult worm was reacted with mouse preimmune sera (**E** and **F**). *nu* nucleus, *em* embryo, *ut* uterus, *mu* muscle, *hm* hemolymp, *in* intestine, *st* stichocyte, *ov* ovary, *o* ova, *s* sperm, *sr* seminal receptacle, *NBL* newborn larvae.

lysate using Co^{2+} affinity chromatography. Nevertheless, rpTsTGH2 was purified at an MW of 45 kDa, whereas rmTsTGH2 was destroyed during purification (data not shown). Thus, purified rpTsTGH2 was employed to determine its effect on activating the human TGF-β signaling pathway using SBE Reporter-HEK293 cells.

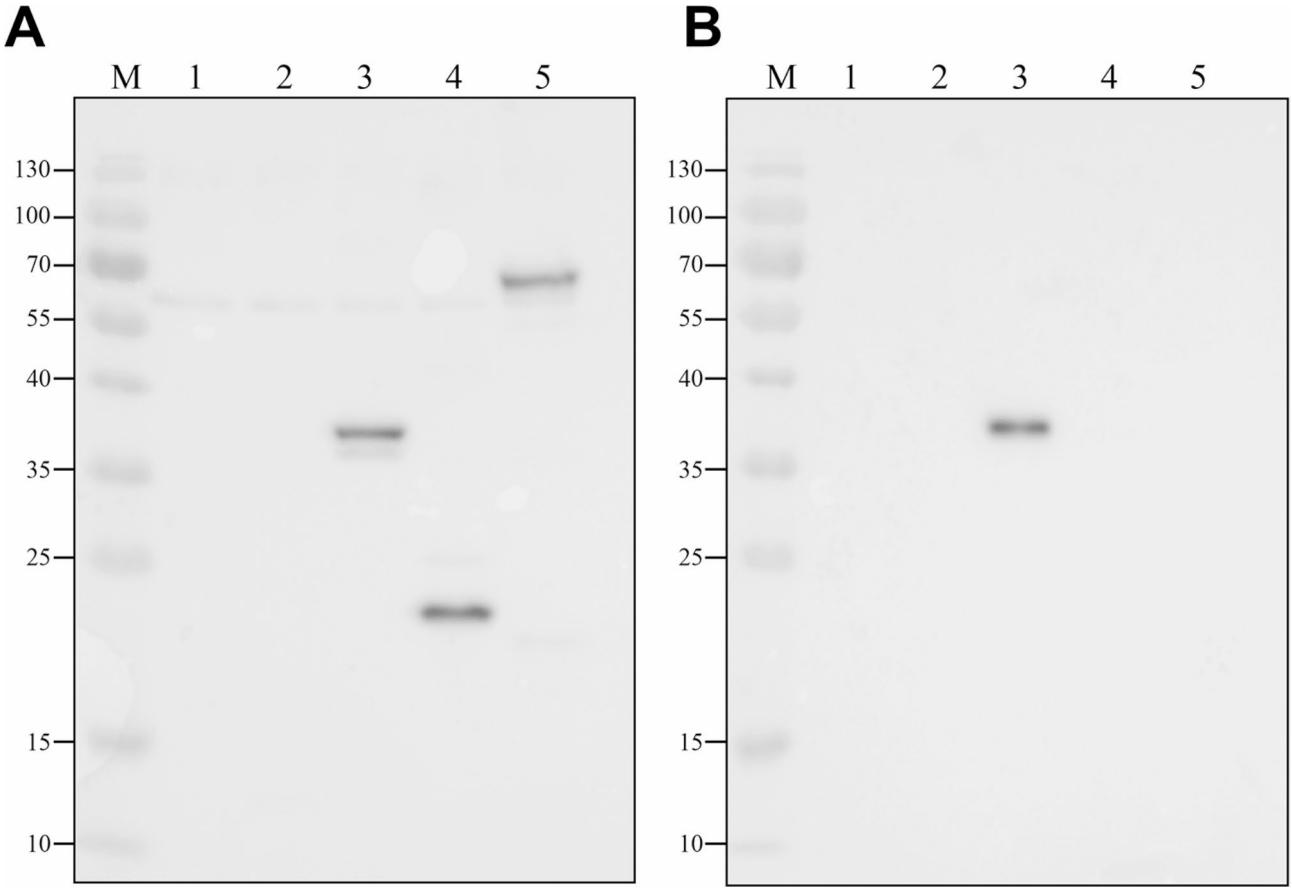

Fig. 8. Expression of recombinant TsTGH2 (rTsTGH2) in mammalian expression system. HEK293T cells were transfected with pSecTag2A carrying pro-TsTGH2 (pSecTag2A/pTsTGH2), pSecTag2A carrying mature-TsTGH-2 (pSecTag2A/mTsTGH2) or pSecTag2A carrying human prostate specific antigen (pSecTag2A/PSA). The rTsTGH2 expression was detected in the cell lysates (**A**) and the culture media (**B**) using western blot probed with mouse anti-His tag antibody. Lane M: PageRuler Prestained Protein Ladder (Thermo Fisher Scientific Inc.); Lane 1: only polyethylenimine [PEI] (Mock transfected); Lane 2: transfected empty pSecTag2A vector (negative control); Lane 3: transfected with pSecTag2A/PSA (positive control); Lane 4: transfected with pSecTag2A/mTsTGH2 and Lane 5: transfected with pSecTag2A/pTsTGH2.

Effect of rpTsTGH2 on activation of the human TGF-β signaling pathway

When rpTsTGH2 was incubated with the SBE Reporter-HEK293 stable cell line, results showed that rpTsTGH2 significantly increased luciferase activity linked to human TGF-β signaling pathway compared to untreated control ($p < 0.05$). Luciferase activity increased when rpTsTGH2 concentration was increased from 1 to 10 ng/mL. When treated with hTGF-β (positive control), luciferase activity was significantly enhanced. rhPSA, an irrelevant control, did not activate luciferase activity in the SBE Reporter-HEK293 stable cell line. The luciferase activity of untreated SBE Reporter-HEK293 cells (negative control) was remarkably low, and the luciferase background was not detectable in the media alone (Fig. 9). SBE Reporter-HEK293 cells treated with cell lysate from HEK293T cells transfected with PEI alone (Mock) and the pSecTag2A vector alone did not activate luciferase activity (Supplementary Information File 2: Fig. S4).

Discussion

TGF-β superfamily comprises many cytokines essential for vertebrate cell and tissue development and differentiation, immune response regulation, tissue healing, bone and cartilage tissue cell activity and metabolism regulation, and bone healing process[48]. In invertebrates, the TGF-β family signaling of the free-living nematode *Caenorhabditis elegans* plays important roles in body size and dauer formation, innate immunity, mesoderm and ectoderm patterning, longevity, and fat metabolism[49]. Likewise, TGF-β has been found in parasitic helminths, and their roles have been described to involve growth and developmental processes. In *F. hepatica*, TGF-β promoted the growth and development of the embryo in the eggs[24]. Apart from controlling the growth and development of parasites, the helminth TGF-β mainly functioned as an immunomodulator to polarize the host immune regulatory responses[20,50–52].

In this study, TGF-β homolog (TsTGH2) from *T. spiralis* was characterized for the first time, and bioinformatics analysis revealed that the domain structure found in TsTGH2 protein consisted of a signal peptide

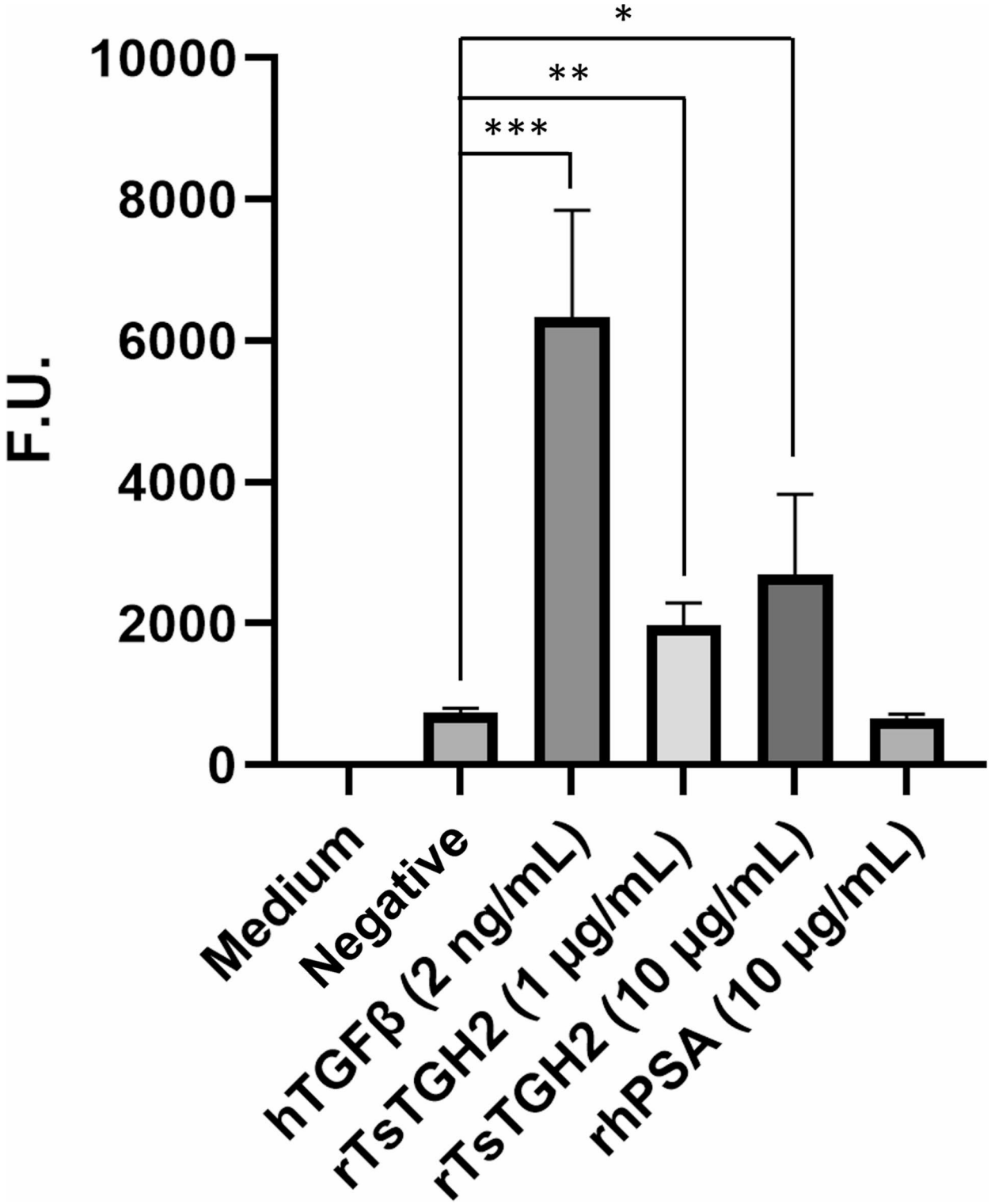

Fig. 9. Effect of recombinant pro-TsTGH2 (rpTsTGH2) on activation of SBE luciferase reporter stable HEK293 cell line. Cells were treated with different concentrations of pTsTGH2 or human TGFβ (hTGFβ). Untreated SBE Reporter-HEK293 cells were used as the negative control. Recombinant human PSA (rhPSA) at 10 µg/mL (rhPSA), serving as an irrelevant control, did not activate luciferase activity. The luciferase activities were measured using a luminometer. Statistical analysis was performed using an unpaired t-test. $^{*}p = 0.0399$; $^{**}p = 0.0028$; $^{***}p = 0.0031$. Data are represented as mean ± SD. The experiments were performed in triplicate and repeated three times.

at the N-terminus, LAP or propeptide portion, and mature protein or TGF-β ligand domain at the C-terminus, similar to the main characteristic of the TGF-β superfamily structure[53]. The signal peptide is highly divergent among TGF-β superfamily members. However, the signal peptide was not observed in some TGF-β homologs of trematodes, such as *S. japonicum*(SjBMP)[23], *S. mansoni*(SmBMP)[22], and *F. hepatica*(FhTLM)[24]. The domain next to the signal peptide is the propeptide portion required for the proper folding and dimerization of mature proteins during biosynthesis[53]. TsTGH2 has a PC cleavage site consisting of RPKR, which is a substrate for proteolytic cleavage to release propeptide from mature TGF-β. The furin cleavage sites in the TGF-β superfamily can have multiple cleavage sites, as found in *Brugia pahangi* TGH1 (RKKR and KRRR)[19] and *S. mansoni* BMP (RKPR, RYKR, RLQR, RSRR, and RHNR)[22]. Several PCs, such as PC1, PC2, furin, PC, PC5, PACE4, and PC7, cleave following a basic residue at either lysine (K) or arginine (R). Most PCs split at the "R/K-Xn-R/K" pattern (where Xn = 0, 2, 4, and 6 amino acid spacer), with arginine being preferred over lysine[53].

A sequence homology comparison between full-length TsTGH2 and other homologs suggested that TsTGH2 has high homology with inhibin members from *Trichinella* species and low homology to TGF-β homologs from other helminths and humans. The mature domain restricted to the C-terminus, which has the highest homology among other domains of the TGF-β superfamily, was used for performing multiple sequence alignment between TsTGH2 and TGF-β homologs. The seven conserved cysteine residues at C_{317}, C_{346}, C_{350}, C_{387}, C_{388}, C_{420}, and C_{422} (Fig. 1A and B) found in the mature protein of TsTGH2 are a signature of the TGF-β superfamily. Two additional conserved cysteines, C_{294} and C_{318}, were also present in TsTGH2, only found in the TGF-β/activin/inhibin subfamily but not in the BMP subfamily. This finding confirmed that TsTGH2 is a member of the TGF-β/activin/inhibin subfamily. In this regard, the conserved cysteines are suggested to be involved in forming disulfide bridges in the cysteine knot, a remarkable feature of the TGF-β superfamily[54].

The phylogenetic tree constructed between TsTGH2 and TGF-β homologs showed that TsTGH2 belonged to the TGF-β/activin/inhibin subfamily, which is located in the same clade as EmAct, SmInAct, and FhINHB-B. Moreover, the tree suggested that TsTGH2 is closely related to the human TGF-β group. In schistosomes, TGF-β like molecules were detected at the surface of cercaria and in the tegument and subsegmental cells of the other stages of *S. japonicum*[55]. *S. mansoni* inhibin/activin (SmInAct) was abundantly expressed in the reproductive tissues of adult females and eggs. Interference of SmInAct gene expression using double-stranded RNA in immature eggs interrupted miracidium development[56]. *E. multicularis* activin A (EmAct) was discovered in metacestode ES products. Recombinant EmAct stimulated T cells to secrete IL-10 and facilitated the expansion of host TGF-β-driven $CD4^+$ $Foxp3^+$ Tregs in vitro[57]. In humans, TGF-β plays a crucial role in regulating immune responses. It inhibits the differentiation of cytotoxic T lymphocytes (CTLs) and T helper 1 (Th1) and Th2 cells, while promoting the generation of peripheral regulatory T cells (Tregs), Th17, Th9, and T follicular helper (Tfh) cells, and facilitates T-cell tissue residence in response to immune challenges[58]. Activins and inhibins are crucial regulators of both innate and adaptive immune responses. Activin A can impair macrophage functions by downregulating the expression of major histocompatibility complex (MHC) class II molecules and decreasing pinocytic and phagocytic activities in lipopolysaccharide (LPS)-treated macrophages, thus reducing their antigen-presenting capabilities[59]. Inhibins influence the induction of Tregs from naïve T cells in the periphery by promoting dendritic cell (DC) maturation and function[60]. In this context, TsTGH2 may possess functions and properties similar to the aforementioned members, providing a basis for further functional analysis. However, the low amino acid homology of TsTGH2 compared to other helminth TGF-β and human TGF-β (less than 30%; Supplementary Information File 1: Table S3) should be taken into account, as it could result in variations in the functions and properties of TsTGH2.

The 2D and 3D protein structures of TsTGH2 were predicted using *S. scrofa* TGF-β1 as the template, and the findings demonstrated that TsTGH2 contains three domains, including a signal peptide, a propeptide domain, and a mature protein domain. The propeptide of TGF-β1 and activin are essential for proper dimerization and folding[61], and the propeptides in BMPs function in targeting the BMP complex (promature domain) to the extracellular matrix[62] and protein stability[63]. The 3D structure of mTsTGH1 contained nine cysteine residues. A rigid structure known as a cysteine knot is created when three disulfide bridges are formed by six cysteine residues. The cysteine knot is involved in locking the bases of several β-sheet strands together and is likely responsible for protein resistance to heat, denaturants, and pH extremes. In addition to six conserved cysteines, the remaining cysteine conserved residues form an additional disulfide bond linking two monomers into a dimer[54]. Moreover, the mature dimeric TGF-β will bind two single-pass transmembrane receptors, TGF-β receptor I (RI) and II (RII), to form a TGF-β signaling pathway[17].

When using mouse anti-rmTsTGH2 pAb, native TsTGH2 was detected in the CSA of ML (L1) and adult *T. spiralis* at an MW of 45 kDa, identical to pTsTGH2. However, mTsTGH2 (17 kDa), which has a lower MW, was not recognized. In this regard, the findings suggested that posttranslational modification or maturation associated with proteolysis may not be necessary for activation. Nevertheless, an in-depth comprehension of TGF-β activation and the TGF-β signaling pathway in the *Trichinella* genus should be elucidated before drawing any conclusions. In other parasites, *Ancylostoma caninum* AcDAF7 was detected in L3 and adult soluble extracts at a band of ~ 40 kDa, representing the unprocessed form containing the ligand domain and propeptide. Anti-AcDAF7 could also detect the mature protein in L3 soluble extracts but not in adult soluble extracts[21]. In *S. mansoni*, anti-SmBMP was recognized in all protein forms in adult male and female worms, including the preprocess form (100 kDa) and two of the process forms (37 and 22 kDa), which have two proteolytic cleavage sites[22]. In addition to CSA, mouse anti-rTsTGH2 pAb detected native TsTGH2 in its unprocessed form in the ES products of adult *T. spiralis*, indicating that TsTGH2 is secreted into the host's environment. However, its roles in regulating host biology, biochemistry, physiology, and immune responses still require extensive evaluation. A previous study demonstrated that TGF-homologs, BmTGH2, detected in the ES product of adult *Brugia malayi*, could bind to the mammalian TGF-β receptor, suggesting that it may promote regulatory T-cell generation[20,64]. *Heligmosomoides polygyrus* TGF-β mimic (Hp-TGM) identified in ES products of the adult parasite interacted

with mammalian TGF-β receptors and induced mouse and human Foxp3$^+$ Treg cell development[50]. In addition to immunomodulation, Hp-TGM promotes tissue regeneration and wound healing in vitro and in vivo[51,65].

T. spiralis expressed TsTGH2 during several stages of development, localizing in distinct tissues at each stage. TsTGH2 expression was detected in the body wall muscle at all developmental stages, suggesting that it may be involved in key development, inducing growth and differentiation. TsTGH2 expression was observed specifically in the ovarian and uterine epithelia of adult *T. spiralis*, as well as in NBL, but not in the embryo. Interestingly, TsTGH2 expression was not observed in the stichosome of AW-6dpi, but TsTGH2 was detected in the ES products of AW-6dpi, unlike AW-3dpi. The presence of TsTGH2 in the uterine epithelia, uterine content, and NBL of AW-6dpi may influence the secretion of TsTGH2 during NBL release. Additionally, the presence of TsTGH2 in ES products, despite being undetectable in the stichosome, may indicate an alternative secretory pathway, such as extracellular vesicles (EVs), for protein secretion. In *H. polygyrus*, EVs contain a TGF-β mimic (TGM) protein, which polarizes naïve peripheral T cells into regulatory T cells (Foxp3$^+$ Tregs)[66]. Isolation of EVs from various developmental stages of *T. spiralis* and subsequent detection of TsTGH2 within these EVs should be conducted to validate this hypothesis.

TGF-β1/LAP expression in the ovarian and uterine epithelia of immature *Onchocerca volvulus* females[67] was consistent with TsTGH2 localization in female reproductive organs in this study. In *Haemonchus contortus*, TGH is located in the body wall muscles, intestine, ovaries of adult females, and testes of adult males. Interference of TGH transcription using specific double-stranded RNA (dsRNA) reduced TGH transcript levels and led to fewer exsheathed third-stage larvae developing into fourth-stage larvae[68]. These findings suggest that TGF-β play a crucial role in the development of genital organs in male and female parasitic nematodes, as well as in embryogenesis and overall parasite development. The roles of TsTGH2 in the reproduction, growth, and development of *T. spiralis* should be thoroughly investigated in future studies. In this regard, RNAi-mediated silencing using siRNA or dsRNA to target TsTGH2 transcription and expression across various developmental stages of the parasite will be prioritized in upcoming research. This approach will facilitate the investigation of TsTGH2's effects on larval survival and infectivity, as well as on the growth, development, reproduction, and embryogenesis of the parasite, ex vivo. Previous studies demonstrated that dsRNA targeting *T. spiralis* serpins (TsSPIs) significantly reduced mRNA and protein expression of the target gene, resulting in a marked decrease in larval invasion and parasite survival within the host[69].

In parasitic helminths, *B. malayi* TGH, BmTGH2, was shown to bind to TGF-β receptor expressing mink lung epithelial cells and activates plasminogen activator inhibitor (PAI)-1 transcription, whereby PAI-1 promotes the recruitment and M2 polarization of monocytes/macrophages[20,70]. *F. hepatica* FhTLM bound to TGF-β receptors RI and RII and mediated downstream signaling through the SMAD2/3-dependent pathway. Treatment of rFhTLM with bovine monocyte-derived macrophages differentiated cells into a regulatory phenotype, which highly expressed IL-10 and Arg-1 and decreased the IL-12 and nitric oxide levels. Furthermore, FhTLM abrogated the antibody-dependent cell cytotoxicity response in vitro[71]. This study demonstrated that the interaction between TsTGH2 and the TGF-β receptor led to rpTsTGH2 slightly activating the TGF-β signaling pathway. However, previous research has shown that only the mature form of TGF-β interacts with its receptor to activate downstream signaling pathways. This is because the N-terminal dimer, known as LAP (latency-associated peptide), forms a ring around the mature TGF-β molecule, effectively masking the interaction site necessary for receptor binding[72]. Consequently, the low activity of rpTsTGH2 may be due to the presence of only trace amounts of its mature form. Additionally, the reduced activity of rTsTGH2 could stem from post-translational modifications that differ between mammalian cell culture and nematode cells, where culture conditions play a critical role in cell function and properties[73]. In this study, rTsTGH2 was also expressed in a prokaryotic system, but the refolded protein was inactive and did not induce TGF-β signaling in the reporter cell. Prokaryotic systems have limitations for expressing helminth recombinant proteins, often leading to improper protein folding, lack of glycosylation (as many helminth antigens carry N- and/or O-glycans), and production in insoluble inclusion bodies, which are challenging to refold[74]. In this context, a prior study demonstrated that the *C. elegans* expression platform can produce functional secretory proteins of parasitic nematodes, confirming that *C. elegans* can generate sufficient quantities of functional proteins suitable for immunological and biochemical studies. Therefore, producing stable rmTsTGH2 and identifying an optimal expression system are urgently needed to accurately assess the activity of TsTGH2, making this a top priority moving forward.

In *T. spiralis* infection, the parasite polarizes macrophages to an alternative phenotype (M2)[75] and suppresses the maturation of dendritic cells[76], reflecting an anti-inflammatory response. In other helminths, these immunomodulatory mechanisms can be induced by TGHs[20,70,71]. However, it is noteworthy that rpTsTGH2 required a significantly higher concentration to interfere with luciferase activity compared to hTGF-β (positive control). This discrepancy may arise because TsTGH2 does not elicit the same immunomodulatory function as other helminthic TGHs, potentially acting as a pathogen-associated molecular pattern (PAMP) instead. Alternatively, differences in protein expression mechanisms or post-translational modifications between the human expression system and the parasitic helminth could also contribute to this observation. Addressing these issues necessitates the purification of native TsTGH2 to comprehensively test its properties and functions. Additionally, optimizing the expression system should be prioritized in the near future.

Conclusions

In this study, TsTGH2, a TGF homolog, was characterized for the first time in *T. spiralis*. Native TsTGH2 was primarily expressed in the body wall muscles of all developmental stages and female reproductive organs. Native TsTGH2 is present in ES products, and its recombinant protein can interact with the human TGF-β receptor to drive downstream signaling through the SMAD2/3-dependent pathway. However, the observed weak induction of the TGF-β signaling pathway may be due to differences in post-translational processing or in vitro culture conditions between mammalian cell culture and parasitic nematodes, which could significantly impact cell

function and properties. Therefore, further research is needed to identify and optimize a suitable expression system or conditions for TsTGH2. Additionally, the functions of native TsTGH2 should be characterized in relation to parasite development and host immunomodulation before drawing conclusions about its precise role.

Data availability

All data generated or analyzed during this study are included in this published article (and its Supplementary Information files).

Received: 30 July 2024; Accepted: 6 December 2024
Published online: 28 December 2024

References

1. Wu, Z., Sofronic-Milosavljevic, L., Nagano, I. & Takahashi, Y. *Trichinella spiralis*: nurse cell formation with emphasis on analogy to muscle cell repair. *Parasit. Vectors* **1**(1), 27 (2008).
2. Jasmer, D. P. & Neary, S. M. *Trichinella spiralis*: inhibition of muscle larva growth and development is associated with a delay in expression of infected skeletal muscle characteristics. *Exp. Parasitol.* **78**(3), 317–325 (1994).
3. Bruschi, F. The immune response to the parasitic nematode *Trichinella* and the ways to escape it. From experimental studies to implications for human infection. *Curr. Drug Targets Immune Endocr. Metabol. Disord.* **2**(3), 269–280 (2002).
4. Motomura, Y. et al. Helminth antigen-based strategy to ameliorate inflammation in an experimental model of colitis. *Clin. Exp. Immunol.* **155**(1), 88–95 (2009).
5. Gruden-Movsesijan, A. et al. *Trichinella spiralis*: modulation of experimental autoimmune encephalomyelitis in DA rats. *Exp. Parasitol.* **118**(4), 641–647 (2008).
6. Saunders, K. A., Raine, T., Cooke, A. & Lawrence, C. E. Inhibition of autoimmune type 1 diabetes by gastrointestinal helminth infection. *Infect. Immun.* **75**(1), 397–407 (2007).
7. Park, H. K., Cho, M. K., Choi, S. H., Kim, Y. S. & Yu, H. S. *Trichinella spiralis*: infection reduces airway allergic inflammation in mice. *Exp. Parasitol.* **127**(2), 539–544 (2011).
8. Kradin, R. L., Badizadegan, K., Auluck, P., Korzenik, J. & Lauwers, G. Y. Iatrogenic *Trichuris suis* infection in a patient with crohn disease. *Arch. Pathol. Lab. Med.* **130**(5), 718–720 (2006).
9. Nagano, I., Wu, Z. & Takahashi, Y. Functional genes and proteins of *Trichinella* spp. *Parasitol. Res.* **104**(2), 197–207 (2009).
10. Bruschi, F. et al. Inhibitory effects of human neutrophil functions by the 45-kD glycoprotein derived from the parasitic nematode *Trichinella spiralis*. *Int. Arch. Allergy Immunol.* **122**(1), 58–65 (2000).
11. Du, L. et al. The protective effect of the recombinant 53-kDa protein of *Trichinella spiralis* on experimental colitis in mice. *Dig. Dis. Sci.* **56**(10), 2810–2817 (2011).
12. Chen, Z. B. et al. Recombinant *trichinella spiralis* 53-kDa protein activates M2 macrophages and attenuates the LPS-induced damage of endotoxemia. *Innate Immun.* **22**(6), 419–432 (2016).
13. Wei, L. Y. et al. Protective effects of recombinant 53-kDa protein of *Trichinella spiralis* on acute lung injury in mice via alleviating lung pyroptosis by promoting M2 macrophage polarization. *Innate Immun.* **27**(4), 313–323 (2021).
14. Kobpornchai, P. et al. A novel cystatin derived from *Trichinella spiralis* suppresses macrophage-mediated inflammatory responses. *PLoS Negl. Trop. Dis.* **14**(4), e0008192 (2020).
15. Tan, T. H. et al. Macrophage migration inhibitory factor of the parasitic nematode *Trichinella spiralis*. *Biochem. J.* **357**(Pt 2), 373–383 (2001).
16. Wu, Z., Boonmars, T., Nagano, I., Nakada, T. & Takahashi, Y. Molecular expression and characterization of a homologue of host cytokine macrophage migration inhibitory factor from *Trichinella* spp. *J. Parasitol.* **89**(3), 507–515 (2003).
17. Chen, W. & Ten Dijke, P. Immunoregulation by members of the TGFβ superfamily. *Nat. Rev. Immunol.* **16**(12), 723–740 (2016).
18. Shi, Y. & Massagué, J. Mechanisms of TGF-beta signaling from cell membrane to the nucleus. *Cell* **113**(6), 685–700 (2003).
19. Gomez-Escobar, N., Lewis, E. & Maizels, R. M. A novel member of the transforming growth factor-beta (TGF-beta) superfamily from the filarial nematodes *Brugia malayi* and *B. pahangi*. *Exp. Parasitol.* **88**(3), 200–209 (1998).
20. Gomez-Escobar, N., Gregory, W. F. & Maizels, R. M. Identification of tgh-2, a filarial nematode homolog of *Caenorhabditis elegans* daf-7 and human transforming growth factor beta, expressed in microfilarial and adult stages of *Brugia malayi*. *Infect. Immun.* **68**(11), 6402–6410 (2000).
21. Brand, A. M., Varghese, G., Majewski, W. & Hawdon, J. M. Identification of a DAF-7 ortholog from the hookworm *Ancylostoma caninum*. *Int. J. Parasitol.* **35**(14), 1489–1498 (2005).
22. Freitas, T. C., Jung, E. & Pearce, E. J. A bone morphogenetic protein homologue in the parasitic flatworm, *Schistosoma mansoni*. *Int. J. Parasitol.* **39**(3), 281–287 (2009).
23. Liu, R. et al. Cloning and characterization of a bone morphogenetic protein homologue of *Schistosoma japonicum*. *Exp. Parasitol.* **135**(1), 64–71 (2013).
24. Japa, O., Hodgkinson, J. E., Emes, R. D. & Flynn, R. J. TGF-β superfamily members from the helminth *Fasciola hepatica* show intrinsic effects on viability and development. *Vet. Res.* **46**, 29 (2015).
25. Pozio, E. & Khamboonruang, C. Trichinellosis in Thailand: epidemiology and biochemical identification of the aethiological agent. *Trop. Med. Parasitol.* **40**(1), 73–74 (1989).
26. Wu, Z., Nagano, I., Takahashi, Y. & Maekawa, Y. Practical methods for collecting *Trichinella* parasites and their excretory-secretory products. *Parasitol. Int.* **65**(5 Pt B), 591–595 (2016).
27. Jiang, P., Wang, Z. Q., Cui, J. & Zhang, X. Comparison of artificial digestion and baermann's methods for detection of *Trichinella spiralis* pre-encapsulated larvae in muscles with low-level infections. *Foodborne Pathog Dis.* **9**(1), 27–31 (2012).
28. Chaimon, S. et al. Molecular characterization and functional analysis of the *Schistosoma mekongi* Ca^{2+}-dependent cysteine protease (calpain). *Parasit. Vectors* **12**(1), 383 (2019).
29. Madeira, F. et al. Search and sequence analysis tools services from EMBL-EBI in 2022. *Nucleic Acids Res.* **50**(W1), W276–w9 (2022).
30. Petersen, T. N., Brunak, S., von Heijne, G. & Nielsen, H. SignalP 4.0: discriminating signal peptides from transmembrane regions. *Nat. Methods* **8**(10), 785–786 (2011).
31. Krogh, A., Larsson, B., von Heijne, G. & Sonnhammer, E. L. Predicting transmembrane protein topology with a hidden Markov model: application to complete genomes. *J. Mol. Biol.* **305**(3), 567–580 (2001).
32. Gupta, R. & Brunak, S. Prediction of glycosylation across the human proteome and the correlation to protein function. *Pac. Symp. Biocomput.* 310–322 (2002).
33. Steentoft, C. et al. Precision mapping of the human O-GalNAc glycoproteome through SimpleCell technology. *Embo J.* **32**(10), 1478–1488 (2013).
34. Duckert, P., Brunak, S. & Blom, N. Prediction of proprotein convertase cleavage sites. *Protein Eng. Des. Sel.* **17**(1), 107–112 (2004).
35. Stothard, P. The sequence manipulation suite: JavaScript programs for analyzing and formatting protein and DNA sequences. *Biotechniques* **28**(6), 1102 (2000).

36. Edgar, R. C. MUSCLE: multiple sequence alignment with high accuracy and high throughput. *Nucleic Acids Res.* **32**(5), 1792–1797 (2004).
37. Tamura, K., Stecher, G. & Kumar, S. MEGA11: Molecular evolutionary genetics analysis version 11. *Mol. Biol. Evol.* **38**(7), 3022–3027 (2021).
38. Laskowski, R. A., Jabłońska, J., Pravda, L., Vařeková, R. S. & Thornton, J. M. PDBsum: structural summaries of PDB entries. *Protein Sci.* **27**(1), 129–134 (2018).
39. Yang, J. & Zhang, Y. I-TASSER server: new development for protein structure and function predictions. *Nucleic Acids Res.* **43**(W1), W174–W181 (2015).
40. Heo, L., Park, H. & Seok, C. GalaxyRefine: protein structure refinement driven by side-chain repacking. *Nucleic Acids Res.* **41**(Web Server issue), W384–W388 (2013).
41. Williams, C. J. et al. MolProbity: more and better reference data for improved all-atom structure validation. *Protein Sci.* **27**(1), 293–315 (2018).
42. Wiederstein, M. & Sippl, M. J. ProSA-web: interactive web service for the recognition of errors in three-dimensional structures of proteins. *Nucleic Acids Res.* **35**(Web Server issue), W407–W410 (2007).
43. Pakchotanon, P. et al. Molecular characterization of serine protease inhibitor isoform 3, SmSPI, from *Schistosoma mansoni*. *Parasitol. Res.* **115**(8), 2981–2994 (2016).
44. Yoonuan, T., Nuamtanong, S., Dekumyoy, P., Phuphisut, O. & Adisakwattana, P. Molecular and immunological characterization of cathepsin L-like cysteine protease of *Paragonimus pseudoheterotremus*. *Parasitol. Res.* **115**(12), 4457–4470 (2016).
45. The enzyme-linked immunosorbent assay (ELISA). *Bull. World Health Organ.* **54**(2), 129–139 (1976).
46. GenSmart™ Codon Optimization Tool. https://www.genscript.com/tools/gensmart-codon-optimization. Accessed 10, 2022.
47. Addgene Generating Stable Cell Lines with Lentivirus. https://www.addgene.org/protocols/generating-stable-cell-lines/. Accessed 25 Feb 2022 (2019).
48. Poniatowski, Ł. A., Wojdasiewicz, P., Gasik, R. & Szukiewicz, D. Transforming growth factor beta family: insight into the role of growth factors in regulation of fracture healing biology and potential clinical applications. *Mediators Inflamm.* **2015**, 137823 (2015).
49. Savage-Dunn, C. & Padgett, R. W. The TGF-β family in *Caenorhabditis elegans*. *Cold Spring Harb. Perspect. Biol.* **9**(6) (2017).
50. Johnston, C. J. C. et al. A structurally distinct TGF-β mimic from an intestinal helminth parasite potently induces regulatory T cells. *Nat. Commun.* **8**(1), 1741 (2017).
51. Lothstein, K. E. et al. A helminth mimic of TGF-β, TGM, enhances regenerative cutaneous wound healing and modulates immune cell recruitment and activation. *bioRxiv* 2022:2022.09.24.509317.
52. Musah-Eroje, M. et al. A host-independent role for *Fasciola hepatica* transforming growth factor-like molecule in parasite development. *Int. J. Parasitol.* **51**(6), 481–492 (2021).
53. Hinck, A. P., Mueller, T. D. & Springer, T. A. Structural biology and evolution of the TGF-β family. *Cold Spring Harb Perspect. Biol.* ;**8**(12) (2016).
54. Kingsley, D. M. The TGF-beta superfamily: new members, new receptors, and new genetic tests of function in different organisms. *Genes Dev.* **8**(2), 133–146 (1994).
55. Hirata, M., Hirata, K., Hara, T., Kawabuchi, M. & Fukuma, T. Expression of TGF-beta-like molecules in the life cycle of *Schistosoma japonicum*. *Parasitol. Res.* **95**(6), 367–373 (2005).
56. Freitas, T. C., Jung, E. & Pearce, E. J. TGF-beta signaling controls embryo development in the parasitic flatworm *Schistosoma mansoni*. *PLoS Pathog.* **3**(4), e52 (2007).
57. Nono, J. K., Lutz, M. B. & Brehm, K. A secreted *Echinococcus multilocularis* activin A homologue promotes regulatory T cell expansion. *bioRxiv* 618140 (2019).
58. Sanjabi, S., Oh, S. A. & Li, M. O. Regulation of the immune response by TGF-β: from conception to autoimmunity and infection. *Cold Spring Harb Perspect. Biol.* **9**(6) (2017).
59. Aleman-Muench, G. R. & Soldevila, G. When versatility matters: activins/inhibins as key regulators of immunity. *Immunol. Cell. Biol.* **90**(2), 137–148 (2012).
60. de la Fuente-Granada, M., Olguín-Alor, R., Ortega-Francisco, S., Bonifaz, L. C. & Soldevila, G. Inhibins regulate peripheral regulatory T cell induction through modulation of dendritic cell function. *FEBS Open. Biol.* **9**(1), 137–147 (2019).
61. Gray, A. M. & Mason, A. J. Requirement for activin A and transforming growth factor-beta 1 pro-regions in homodimer assembly. *Science* **247**(4948), 1328–1330 (1990).
62. Gregory, K. E. et al. The prodomain of BMP-7 targets the BMP-7 complex to the extracellular matrix. *J. Biol. Chem.* **280**(30), 27970–27980 (2005).
63. Constam, D. B. & Robertson, E. J. Regulation of bone morphogenetic protein activity by pro domains and proprotein convertases. *J. Cell. Biol.* **144**(1), 139–149 (1999).
64. McSorley, H. J., Harcus, Y. M., Murray, J., Taylor, M. D. & Maizels, R. M. Expansion of $Foxp^{3+}$ regulatory T cells in mice infected with the filarial parasite *Brugia malayi*. *J. Immunol.* **181**(9), 6456–6466 (2008).
65. Redgrave, R. E. et al. Exogenous transforming growth factor-β1 and its helminth-derived mimic attenuate the heart's inflammatory response to ischemic injury and reduce mature scar size. *Am. J. Pathol.* (2023).
66. Drurey, C. & Maizels, R. M. Helminth extracellular vesicles: interactions with the host immune system. *Mol. Immunol.* **137**, 124–133 (2021).
67. Korten, S. et al. The nematode parasite *Onchocerca volvulus* generates the transforming growth factor-beta (TGF-beta). *Parasitol. Res.* **105**(3), 731–741 (2009).
68. He, L. et al. A daf-7-related TGF-β ligand (Hc-tgh-2) shows important regulations on the development of *Haemonchus contortus*. *Parasit. Vectors* **13**(1), 326 (2020).
69. Yi, N. et al. RNAi-mediated silencing of *Trichinella spiralis* serpin-type serine protease inhibitors results in a reduction in larval infectivity. *Vet. Res.* **51**(1), 139 (2020).
70. Kubala, M. H. et al. Plasminogen activator inhibitor-1 promotes the recruitment and polarization of macrophages in cancer. *Cell. Rep.* **25**(8), 2177–91e7 (2018).
71. Sulaiman, A. A. et al. A trematode parasite derived growth factor binds and exerts influences on host immune functions via host cytokine receptor complexes. *PLoS Pathog.* **12**(11), e1005991 (2016).
72. Liénart, S. et al. Structural basis of latent TGF-β1 presentation and activation by GARP on human regulatory T cells. *Science* **362**(6417), 952–956 (2018).
73. Khan, K. H. Gene expression in mammalian cells and its applications. *Adv. Pharm. Bull.* **3**(2), 257–263 (2013).
74. Geldhof, P., De Maere, V., Vercruysse, J. & Claerebout, E. Recombinant expression systems: the obstacle to helminth vaccines? *Trends Parasitol.* **23**(11), 527–532 (2007).
75. Bai, X. et al. Regulation of cytokine expression in murine macrophages stimulated by excretory/secretory products from *Trichinella spiralis* in vitro. *Mol. Cell. Biochem.* **360**(1–2), 79–88 (2012).
76. Langelaar, M. et al. Suppression of dendritic cell maturation by *Trichinella spiralis* excretory/secretory products. *Parasite Immunol.* **31**(10), 641–645 (2009).

Acknowledgements
We gratefully thank the Department of Helminthology, Faculty of Tropical Medicine, Mahidol University for supporting all facilities and manpower in this study. Our gratitude also goes to the Thammasat University Research Unit in Nutraceuticals and Food Safety, and the Research Group in Medical Biomolecules, Faculty of Medicine, Thammasat University for facilitating us all necessary instruments and services.

Author contributions
SC, OP, PM, and PAD conceived and designed the study. OP, PML, WM, LS, and PAD maintained *T. spiralis* life cycle. SC, OP, OR, SS, and PAD performed bioinformatics and molecular characterizations. SC, PML and PAD involved in immunological technique and analysis. SC, KF and SA performed immunolocalization. SC, OR, OP, PC, PM and PAD analyzed the data and results. SC, OP and PAD drafted the manuscript. OP, OR, PC, JT, WM, PM and PAD helped in comments and discussions. All authors read and approved the final manuscript.

Funding
This study was supported by TRF Research Career Development Grant and Mahidol University through Dr. Poom Adisakwattana (RSA6180072), the Thailand Science Research and Innovation Fundamental Fund (Grant number TUFF32/2565), the Thammasat University Research Grant (Contract no. TUFT-FF27/2565), and the National Research Council of Thailand (NRCT): High-Potential Research Team Grant Program (Contract no. N42A670561 to WM).

Declarations

Competing interests
The authors declare no competing interests.

Ethics approval and consent to participate
All procedures performed on animals in this study were conducted following the ethical principles and guidelines for the use of animals at the National Research Council of Thailand (NRCT) and with permission from the Faculty of Tropical Medicine Animal Care and Use Committee (FTM-ACUC), Mahidol University, with approval number FTM-ACUC 018/2021.

Additional information
Supplementary Information The online version contains supplementary material available at https://doi.org/10.1038/s41598-024-82599-x.

Correspondence and requests for materials should be addressed to P.M. or P.A.